

# Basic Study on Ecological Adaptive Cruise Control for Electric Delivery Trucks Considering Cornering Resistance by Dynamic Programming and State Feedback Control

Yuki Hosomi <sup>*a)</sup>	Student Member,	Binh Minh Nguyen <sup>*</sup>	Member
Hiroshi Fujimoto <sup>*</sup>	Senior Member,	Kenji Yaguchi <sup>**</sup>	Non-member
Yoshihiro Inoue <sup>**</sup>	Non-member		

Electric vehicles are becoming more popular worldwide, not only for passenger vehicles but also for commercial vehicles such as delivery trucks. The demand for extending the cruising range per charge is significant, and improving energy efficiency while driving is essential for delivery trucks in urban areas. This study proposes an ecological adaptive cruise control method combining offline dynamic programming and online state feedback control to achieve tracking performance and energy efficiency with a low computational burden. Offline dynamic programming generates optimal speed trajectory considering road grade and cornering. The online state feedback controller considers the constraint from the preceding vehicle. Simulations show that the proposed method is more ecological than the constant speed controller. In addition, actual vehicle experiments show that it is possible to achieve both tracking performance and energy efficiency by tuning the weight of the state feedback controller.

**Keywords:** electric delivery truck, adaptive cruise control, energy reduction, dynamic programming, cornering resistance

## 1. Introduction

Electrification of vehicles is progressing worldwide<sup>(1)</sup>. Electric vehicles are also appearing in delivery trucks. However, there is still the issue of electric vehicles' cruising range limitation. Delivery trucks are heavier than passenger vehicles and have a large auxiliary power consumption, such as refrigerators. Thus, improving driving energy efficiency is essential to enhance practicality. On the other hand, electric vehicles have achieved advanced motion control by using the high responsiveness of electric motors<sup>(2)</sup>. Many control methods have been proposed to improve energy efficiency, including energy-efficient torque vectoring<sup>(3)(4)</sup>, driving force distribution<sup>(5)</sup>, and optimal speed control<sup>(6)(7)</sup>. Taking advantage of the above characteristics, this study proposes an optimal speed control method for battery electric delivery trucks (EDT).

As for the optimal speed control of electric vehicles, there are two types of research: optimal speed trajectory considering road shape<sup>(8)(9)</sup> and adaptive cruise control<sup>(7)(10)</sup>. As for the optimal speed trajectory considering road shape, several studies consider road grade and cornering<sup>(8)(9)</sup>. However, they all assume an environment with no surrounding vehicles. In the case of adaptive cruise control, the prediction of the behavior of the preceding vehicle and the real-time computational burden are issues<sup>(11)-(15)</sup>. Most adaptive cruise controllers in practical use are implemented by state feedback control and

do not optimize for road geometry<sup>(16)</sup>. There is research on the quadrant dynamic programming that suppresses the computational burden in adaptive cruise control. However, it does not consider the optimization for road shape<sup>(7)</sup>. In addition, optimizing the preceding vehicle and the gradient by the model predictive control of the preceding vehicle following has been studied<sup>(10)</sup>. However, the issue of high real-time computational burden remains.

To address the above issues, this study proposes an ecological adaptive cruise control method combining dynamic programming and state feedback control. The contribution of this study is that the optimization for road shape before driving and the real-time adaptive cruise control are realized by dynamic programming and the state feedback control, respectively. It suppresses the real-time computational burden and realizes tracking performance and energy efficiency by considering road shape. Moreover, this study considers and uses the detailed EDT energy model containing the cornering resistance, regenerative torque limitation, and motor efficiency maps. In the simulation, the energy consumption of the proposed method is compared with that of constant speed control. The simulation results confirmed that the proposed method improves energy efficiency. Actual vehicle experiments are conducted to evaluate the tracking and energy performance when changing the weight of the state feedback control. The results show that changing the weight of the state feedback control can achieve the desired performance.

The remainder of this paper is organized as follows. In the next section, we explain the energy model of EDTs. In the third section, the problem setting is defined. In the fourth section, the proposed method of the combination of dynamic

a) Correspondence to: hosomi.yuki22@ae.k.u-tokyo.ac.jp

\* The University of Tokyo

5-1-5, Kashiwanoha, Kashiwa, Chiba, 277-8561 Japan

\*\* Mitsubishi Fuso Truck and Bus Corporation

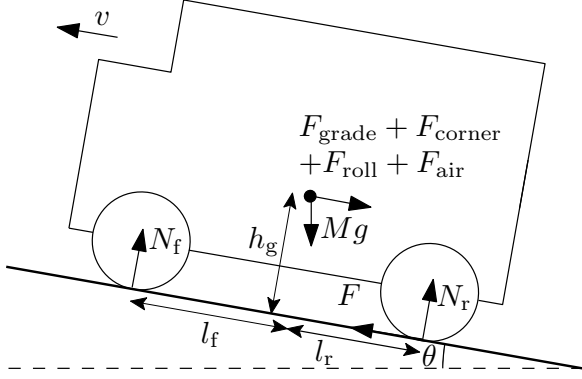


Figure 1: Modeling of an EV with a rear on-board motor.

programming and state feedback control is clarified. In the fifth and sixth sections, we validate the proposed method in the simulation and actual vehicle experiments.

## 2. Modeling

**2.1 Vehicle Dynamics** The vehicle dynamics of the EDT are modeled as shown in Fig. 1. The single-wheel model is used and expressed by the following equations.

$$M \frac{dv}{dt} = F - F_{DR}, \quad (1)$$

where  $F$ ,  $F_{DR}$ ,  $v$ , and  $M$  are the driving force, resistance force, vehicle speed, and vehicle mass, respectively.

The resistance force is defined as the sum of air  $F_{air}$ , rolling  $F_{roll}$ , grade  $F_{grade}$ , and cornering  $F_{corner}$  resistance<sup>(9)</sup>.

$$F_{DR} = F_{air} + F_{roll} + F_{grade} + F_{corner} \quad (2)$$

$$F_{air} = cv^2 \quad (3)$$

$$F_{roll} = \mu Mg \cos \theta \quad (4)$$

$$F_{grade} = Mg \sin \theta \quad (5)$$

$$F_{corner} \approx \frac{M^2}{2(l_f + l_r)^2} \left( \frac{l_r^2}{C_f} + \frac{l_f^2}{C_r} \right) \frac{v^4}{R^2} \quad (6)$$

where  $c$ ,  $\mu$ ,  $\theta$ ,  $l_f$ ,  $l_r$ ,  $C_f$ ,  $C_r$ , and  $R$  are the air resistance and rolling resistance coefficient, slope angle, distance from the center of gravity to front and rear axle, cornering stiffness of front and rear, and cornering radius respectively.

Considering the gear ratio and loss, the motor torque  $T$  and speed  $\omega$  are expressed as follows:

$$T = \begin{cases} \frac{rF}{g_e g_r} & (\dot{v} \geq 0) \\ \frac{g_e r F}{g_r} & (\dot{v} < 0) \end{cases}, \quad (7)$$

$$\omega = \frac{g_r v}{r}, \quad (8)$$

where  $r$ ,  $g_r$ , and  $g_e$  are the wheel radius, gear ratio, and transmission efficiency, respectively.

**2.2 Energy Model** Motor torque, speed, and efficiency maps are used for the energy model. From efficiency maps of motor torque and speed as energy models, the energy consumption is calculated by the product of the efficiency  $\eta$  and output power  $\omega T$ . Since the regenerative torque is limited at each motor speed  $T_{min}(\omega)$ , the inverter input power  $P_{in}$

is formulate as follows:

$$P_{in} = \begin{cases} \eta(\omega, T) \omega T & (0 \leq T) \\ \frac{\omega T}{\eta(\omega, T)} & (T_{min}(\omega) < T < 0) \\ \frac{\omega T_{min}}{\eta(\omega, T_{min})} & (T \leq T_{min}(\omega)) \end{cases} \quad (9)$$

The energy consumption can be calculated by the vehicle speed and acceleration from these vehicle dynamics and energy models.

## 3. Problem Formulation

This study assumes an environment where EDT follows the preceding vehicle. The optimization focuses on the constraints from the preceding vehicle and road geometry and does not consider other constraints, such as traffic signals. It is assumed that the vehicle speed  $v_f$  and position  $x_f$  are obtained from the vehicle Controller Area Network (CAN) and GPS. The distance  $d$  between the preceding and target vehicle is assumed to be obtained from the millimeter wave radar. The preceding vehicle's speed  $v_p$  and position  $x_p$  can be estimated from the distance  $d$  and the own vehicle states ( $v_f$ ,  $x_f$ ). Assuming that the operating route is determined before driving, offline optimization is implemented before driving, and only the optimized results are given to the EDT.

## 4. Proposed Method

**4.1 Overall System** Figure 2 shows an overview of the proposed method. An optimal speed trajectory is generated offline considering the road shape, such as road grade and corner. While driving, the speed reference value is obtained from the preceding vehicle's speed and the vehicle's position. Finally, the motor torque reference is implemented by state feedback control by using the two states of the speed and distance.

**4.2 Dynamic Programming** Dynamic programming discretized in speed, position, and time for offline optimal speed trajectory generation considering road shape is used<sup>(17)(18)</sup>. The objective function uses total energy consumption, which is expressed as the sum of the inverter input power  $P_{in}$  and the auxiliary power  $\alpha$ . The energy and motor torque are calculated from the obtained vehicle and energy model with the speed trajectory as a variable. The motor torque is limited by considering the regenerative torque limit, and the acceleration constraint is also used to prevent cargo collapse. The initial and terminal speeds are set to the same constant value  $v_{con}$  as the preceding vehicle by selecting starting and ending points with no road grade or corner. For tracking purposes, the time required within a section is matched to the case of constant speed driving at  $v_{con}$ . In order to cope with changes in the preceding vehicle's speed, dynamic programming optimization is performed for all possible  $v_{con}$ .

$$\min_{v_f(k)} \sum_{k=0}^L (P_{in}(k) \Delta t + \alpha \Delta t), \quad (10)$$

$$\text{s.t.: } x_f(k+1) = x_f(k) + \frac{v_f(k+1) + v_f(k)}{2} \Delta t, \quad (11)$$

$$a(k) = \frac{v_f(k+1) - v_f(k)}{\Delta t}, \quad (12)$$

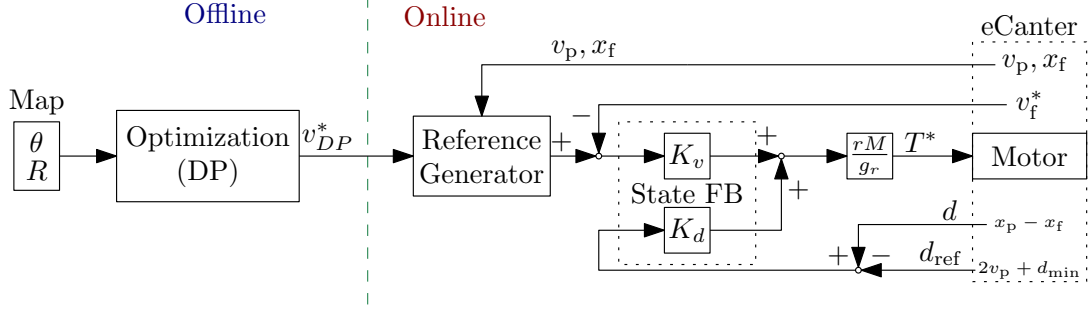


Figure 2: Overall control block diagram of the proposed system.

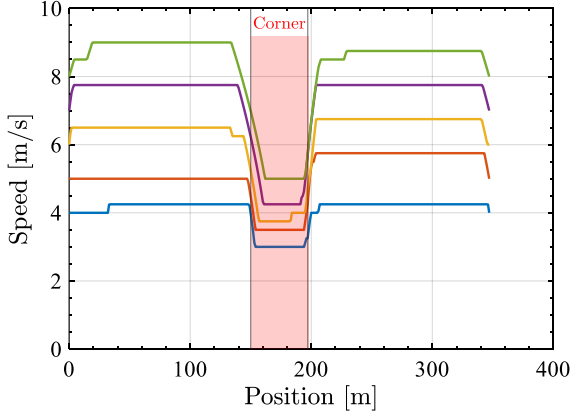


Figure 3: Generated optimal speed trajectory.

$$T_{\min} \leq T(k) \leq T_{\max}, \quad (13)$$

$$a_{\min} \leq a(k) \leq a_{\max}, \quad (14)$$

$$v(0) = v_{\text{con}}, v(L) = v_{\text{con}}, L = d/v_{\text{con}} \quad (15)$$

$$\text{Eqs. (1), (7) - (9)}. \quad (16)$$

Figure 3 shows the generated optimal speed trajectories at each constant speed  $v_{\text{con}}$  from 4 m/s to 9 m/s.

**4.3 Online Reference Generator** For speed reference, the optimal speed at each point in the two-dimensional plane of the preceding vehicle's speed and own vehicle's position is obtained by interpolating the optimal speed trajectory for each preceding vehicle's speed  $v_{\text{con}}$  obtained by dynamic programming. While driving, the preceding vehicle's speed and the vehicle's position are input into the generated map to obtain the optimal speed as a speed reference.

To maintain the time between vehicles, distance reference is determined by the preceding vehicle's speed and the minimum distance  $d_{\min}$ .

$$d_{\text{ref}} = 2v_p + d_{\min} \quad (17)$$

**4.4 State Feedback Control** State feedback control is used to suppress the real-time computational burden. The states are the speed and the distance between the preceding vehicle. The output of the state feedback control is the acceleration, and when converting the acceleration to the motor torque, the resistance force and transmission loss are ignored, and the gear ratio, radius, and vehicle weight are used to determine the motor torque.

$$a^* = K_v(v_{\text{ref}} - v_f) + K_d(d - d_{\text{ref}}) \quad (18)$$

$$T^* = a^* \frac{rM}{g_r} \quad (19)$$



Figure 4: Verification EDT (eCanter).

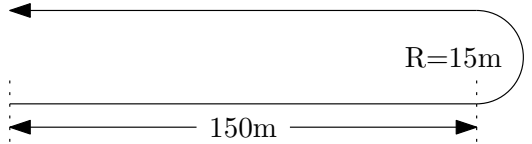


Figure 5: Verification roads.

## 5. Simulation

**5.1 Simulation Setup** In the simulation and experiments, eCanter is used as the verification vehicle, as shown in Fig. 4. eCanter is an EDT manufactured by Mitsubishi Fuso Truck and Bus Corporation. The road conditions for verification are shown in Fig. 5. The gradient can be ignored due to the constraints of the experiment site, and the road shape consists only of straight and turning. The straight is 150 m, and the turning is a circular arc with a radius of 15 m. The vehicle enters the straight section after reaching the same constant speed as the preceding vehicle and runs a route consisting of straight-turn-straight. The speed is set to be the same at the start and end points.

For the validation of the proposed method, the comparison between the proposed method  $K_d = 0.01$ ,  $K_v = 0.3$  and the constant speed control when the preceding vehicle runs at a constant speed of 6 m/s is performed. In the simulation, the acceleration is controlled by the speed controller until both vehicles reach 6 m/s, and the proposed control is started after the speed of the preceding vehicle and the target vehicle are both constant at 6 m/s.

**5.2 Simulation Results** Figures. 6(a) and 6(b) show the vehicle speed and trajectories of the preceding and target vehicles. Figs. 6(c), 6(d), 6(e), and 6(f) show the distance between the preceding vehicle and the target vehicle, motor torque, motor power, and energy consumption trajectories.

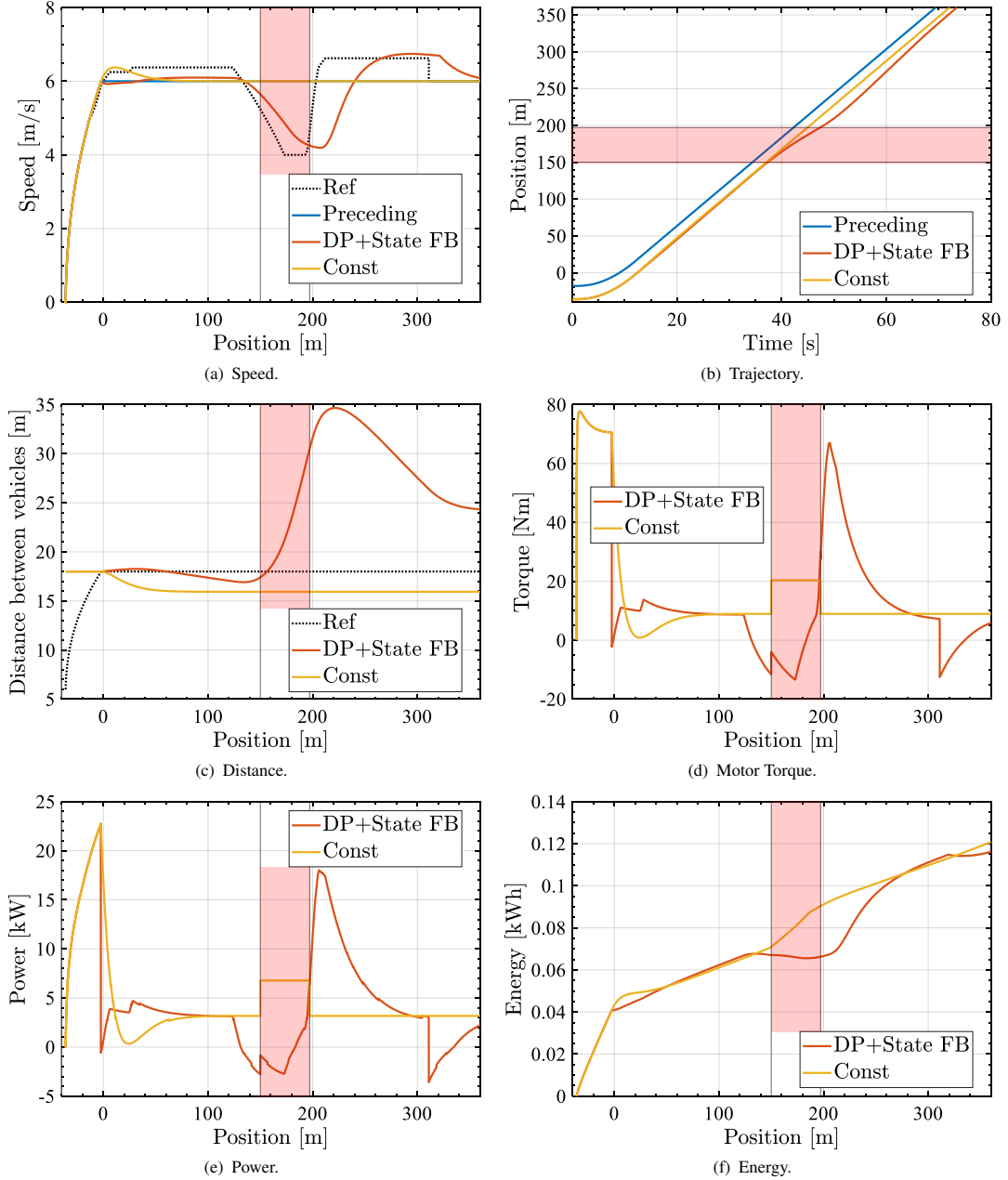


Figure 6: Simulation results. Comparison of power consumption and tracking performance between the proposed method and the method with constant speed trajectory.

The vehicle starts to turn at 150 m after 36 m acceleration and 150 m straight section, and the proposed method reduces energy consumption by decelerating (Figs. 6(e) and 6(f)). Using the proposed method, the vehicle accelerates in a straight line after the corner to reduce the distance between vehicles. Due to the high weighting of speed in the state feedback, the speed reference value is highly tracked, while the distance between vehicles is highly variable, as shown in Figs. 6(a) and 6(c).

## 6. Real Vehicle Experiments

**6.1 Experimental Setup** In the actual vehicle experiments, eCanter is used. The experiment was conducted with the eCanter in an empty state, and the proposed controller is implemented in the dSPACE MicroAutoBox. The motor

torque reference is sent from the MicroAutoBox to the actual vehicle experiment by CAN communication every 10 ms. The energy consumption is measured from vehicle CAN. The road conditions are the same as in the simulation, and a human driver operates the steering to follow the existing white line at the test site.

For comparison, the gains of the state feedback controller change as shown in Table 1. We compare these three cases to compare the effectiveness of the state feedback. Case 1 is balanced with the distance and speed tracking. Case 2 emphasizes the distance, and Case 3 focuses on speed tracking.

**6.2 Experimental Results** Figures 7(a) and 7(b) show the vehicle speed trajectories of the preceding and target vehicles of all three cases. Figs. 7(c), 7(d), 7(e), and

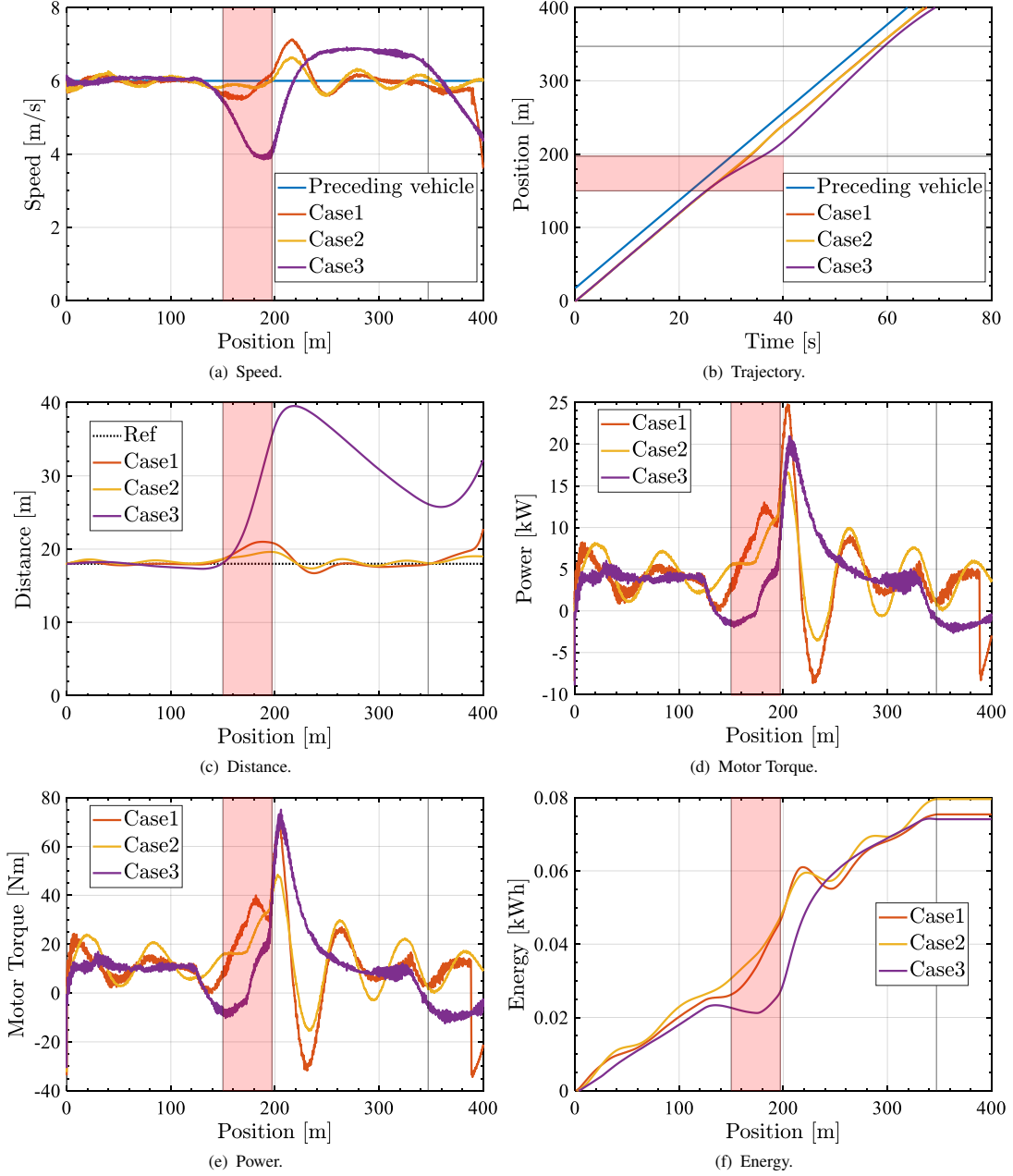


Figure 7: Experimental result. Comparison of behavior at different state feedback gain  $K_v$  and  $K_d$ .

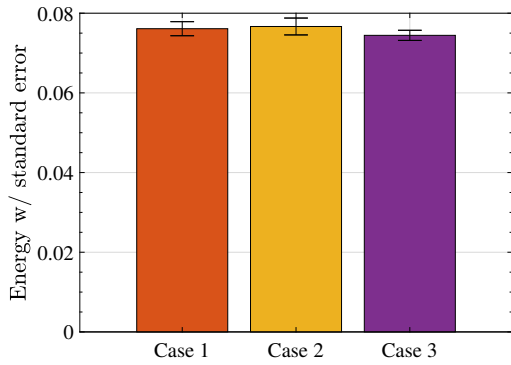


Figure 8: Average energy consumption comparison of three cases.

Table 1: Verification cases in experiments.

Case	Description
1	$K_d = 0.3, K_v = 0.3$
2	$K_d = 0.3, K_v = 0.1$
3	$K_d = 0.1, K_v = 0.3$

7(f) show the distance between the preceding vehicle and the target vehicle, motor torque, motor power, and total energy consumption of three cases.

In Case 3, where the speed weights are more significant, the distance between vehicles fluctuates more. However, the energy consumption is minimal. In Cases 1 and 2, the weights of distance are large. Even though energy consumption is large, they show good tracking performance compared to the preceding vehicle.

Figure 8 shows the average energy consumption of the

three cases. It is confirmed that Case 3, which has the highest weight for following the speed reference value from dynamic programming, has the lowest energy consumption.

## 7. Conclusion

This study proposed an ecological adaptive cruise control system that combines dynamic programming and state feedback control. Offline, the optimal speed trajectory is generated considering a detailed energy model, including cornering resistance, and online, state feedback control is proposed to adjust energy consumption and following performance easily according to the driver's preference and situation. Simulation and actual vehicle experiments showed that both tracking performance and energy efficiency can be achieved by weighting the state feedback control. It is also confirmed that energy consumption can be reduced compared to constant speed when energy is emphasized by the proposed method.

Future work will include verification of the effectiveness of both cornering and road grade. We would also analyze the stability of the closed loop system, discuss the string stability for safety, and propose optimization methods, including traffic signals that could not be considered in this proposal.

## References

- (1) S. Oki and Y. Sato, "Nissan leaf and e-power: Evolution of motors and inverters," *IEEJ Journal of Industry Applications*, vol. 13, no. 1, pp. 8–16, 2024.
- (2) T. Suzuki, M. Mae, T. Takeuchi, H. Fujimoto, and E. Katsuyama, "Model-based filter design for triple skyhook control of in-wheel motor vehicles for ride comfort," *IEEJ Journal of Industry Applications*, vol. 10, no. 3, pp. 310–316, 2021.
- (3) M. Dalboni, D. Tavernini, U. Montanaro, A. Soldati, C. Concarì, M. Dhaens, and A. Sorniotti, "Nonlinear model predictive control for integrated energy-efficient torque-vectoring and anti-roll moment distribution," *IEEE/ASME Transactions on Mechatronics*, vol. 26, no. 3, pp. 1212–1224, 2021.
- (4) N. Guo, X. Zhang, Y. Zou, B. Lenzo, G. Du, and T. Zhang, "A supervisory control strategy of distributed drive electric vehicles for coordinating handling, lateral stability, and energy efficiency," *IEEE Transactions on Transportation Electrification*, vol. 7, no. 4, pp. 2488–2504, 2021.
- (5) H. Fujimoto and S. Harada, "Model-based range extension control system for electric vehicles with front and rear driving-braking force distributions," *IEEE Transactions on Industrial Electronics*, vol. 62, no. 5, pp. 3245–3254, 2015.
- (6) M. Hattori, H. Fujimoto, Y. Hori, Y. Takeda, and K. Sato, "Simple tuning and low-computational-cost controller for enhancing energy efficiency of autonomous-driving electric vehicles," *IEEJ Journal of Industry Applications*, vol. 9, no. 4, pp. 358–365, 2020.
- (7) M. Hattori, O. Shimizu, S. Nagai, H. Fujimoto, K. Sato, Y. Takeda, and T. Nagashio, "Quadrant dynamic programming for optimizing velocity of ecological adaptive cruise control," *IEEE/ASME Transactions on Mechatronics*, vol. 27, no. 3, pp. 1533–1544, 2022.
- (8) H. Yoshida, H. Fujimoto, D. Kawano, Y. Goto, M. Tsuchimoto, and K. Sato, "Range extension autonomous driving for electric vehicles based on optimal velocity trajectory and driving braking force distribution considering road gradient information," in *IECON 2015 - 41st Annual Conference of the IEEE Industrial Electronics Society*, pp. 004754–004759, 2015.
- (9) Y. Ikezawa, H. Fujimoto, D. Kawano, Y. Goto, M. Tsuchimoto, and K. Sato, "Fundamental research on range extension autonomous driving for electric vehicle based on optimization of vehicle velocity profile in consideration of cornering," in *The 29th International Electric Vehicle Symposium and Exhibition*, pp. 1–12, 2016.
- (10) Y. Zhang, X. Qu, and L. Tong, "Optimal eco-driving control of autonomous and electric trucks in adaptation to highway topography: Energy minimization and battery life extension," *IEEE Transactions on Transportation Electrification*, vol. 8, no. 2, pp. 2149–2163, 2022.
- (11) Z. Wang, G. Wu, P. Hao, and M. J. Barth, "Cluster-wise cooperative eco-approach and departure application for connected and automated vehicles along signalized arterials," *IEEE Transactions on Intelligent Vehicles*, vol. 3, no. 4, pp. 404–413, 2018.
- (12) S. Wang and X. Lin, "Eco-driving control of connected and automated hybrid vehicles in mixed driving scenarios," *Applied Energy*, vol. 271, p. 115233, 2020.
- (13) Z. Wang, G. Wu, and M. J. Barth, "Cooperative eco-driving at signalized intersections in a partially connected and automated vehicle environment," *IEEE Transactions on Intelligent Transportation Systems*, vol. 21, no. 5, pp. 2029–2038, 2020.
- (14) Z. Bai, P. Hao, W. ShangGuan, B. Cai, and M. J. Barth, "Hybrid reinforcement learning-based eco-driving strategy for connected and automated vehicles at signalized intersections," *IEEE Transactions on Intelligent Transportation Systems*, vol. 23, no. 9, pp. 15850–15863, 2022.
- (15) M. F. Ozkan and Y. Ma, "Distributed stochastic model predictive control for human-leading heavy-duty truck platoon," *IEEE Transactions on Intelligent Transportation Systems*, vol. 23, no. 9, pp. 16059–16071, 2022.
- (16) K. Hidaka, H. Kitaoka, K. Kitahama, M. Shida, H. Fujimoto, N. Kisu, H. Koike, J. Eguchi, H. Kaseyama, and T. Kato, "Smooth traffic flow using acc in sag section of expressway," *Transactions of the Society of Automotive Engineers of Japan*, vol. 44, no. 2, pp. 765–770, 2013.
- (17) Y. Hosomi, S. Yamada, B.-M. Nguyen, S. Nagai, and H. Fujimoto, "Basic study on energy-optimized speed trajectory for electric vehicles between traffic signals based on stochastic model using low frequency floating car data," in *IEEJ International Workshop on Sensing, Actuation, Motion Control, and Optimization*, pp. 1–6, 2023.
- (18) Y. Hosomi, B.-M. Nguyen, S. Nagai, and H. Fujimoto, "Learning-based distributed approach to energy-optimized speed trajectory for electric vehicles at multiple signalized intersections," in *IECON 2023- 49th Annual Conference of the IEEE Industrial Electronics Society*, pp. 1–6, 2023.